

---

## A Simple Approach to Neutrino Production of $\Delta$ Resonance

---

Ji Young YU

*Theoretische Physik III, University of Dortmund, 44221 Dortmund, Germany*

---

### Abstract

We present a simple and self-contained approach to resonance production by neutrinos focusing on the  $\Delta(1232)$  resonance which is dominant at low energies. In this paper, we consider free nucleon targets. The  $\Delta$  resonance can be described by two form factors  $C_3^V$  and  $C_5^A$ . Using up-to-date parameterizations for these form factors, differential cross sections are calculated and compared with experimental data. Further, we apply this approach to the electroproduction case and calculate pion angular distributions which are compared with experimental data.

### 1. Introduction

Neutrino oscillations are well-established by now pointing to a picture with three massive neutrinos. The oscillations with three neutrino generations are described in terms of three mixing angles  $\theta_{12}, \theta_{13}, \theta_{23}$ , a CP violating phase  $\delta$  and two mass differences  $\Delta_{21} = m_2^2 - m_1^2$ ,  $\Delta_{32} = m_3^2 - m_2^2$ . So far, atmospheric neutrino data and results from the K2K long-baseline (LBL) experiment determine the parameter  $\Delta_{32} = 2.2 \times 10^{-3} \text{ eV}^2$  to about 25% accuracy and the mixing angle  $\theta_{23} \simeq \pi/2$ . An immediate goal of operating and future LBL experiments will be to significantly improve the precision of these determinations. Ultimately, future LBL experiments aim at measuring subdominant oscillation parameters like the mixing angle  $\theta_{13}$  and, if  $\theta_{13}$  is not too small, CP violation in the leptonic sector. For a recent overview see, e.g., Ref. [1]. The typical incoming neutrino fluxes of the LBL experiments are in the sub-GeV up to a few GeV range, similar to the atmospheric neutrino flux. Obviously, with increasing precision of measurements and smallness of parameters it will be necessary to further improve the knowledge of neutrino cross sections used to detect the neutrino species at the near and far detectors of LBL experiments.

The excitation of the resonances by electrons and neutrinos has been studied extensively in the literature. The earlier articles [2, 3, 4, 5, 6] tried to determine

the  $p\Delta$  transition form factors in terms of basic principles, like conserved vector current (CVC), partially conserved axial-vector current (PCAC), dispersion relations, etc. These and subsequent papers introduced dipole form factors and in various cases other functional forms with additional kinematic factors in order to reproduce the data. As a result, the cross sections (differential and integrated) were presented in terms of several parameters [7, 8, 9, 10]. The relatively large number of parameters and the limited statistics of the experiments provided qualitative comparisons but an accurate determination of the terms is still missing.

Therefore, it is important to improve the calculation of the excitation of resonances with isospin  $I = 3/2$  and  $I = 1/2$  looking into various terms that enter the calculations and trying to determine them, as accurately as possible. This has been done recently in Ref. [11]. In this contribution we will focus on the excitation of the  $\Delta$  resonance ( $P_{33}(1232)$ ) which is dominant at the low energies considered here [11] and which is relevant for the study of single pion production in current and future long baseline experiments like K2K, MINOS, OPERA, ICARUS, J2K, etc. The formulas and form factors for other resonances  $P_{11}(1440)$ ,  $S_{11}(1535)$  and  $D_{13}(1520)$  can be found in [11].

In order to obtain larger event rates neutrino experiments use medium-heavy and heavy nuclei targets which brings in additional corrections such as the Pauli exclusion principle, Fermi motion and absorption and charge exchange of the produced pions in nuclei. In this paper, we consider free nucleon targets. For a discussion of nuclear effects included in our approach we refer to Refs. [12].

The paper is organized as follows. In Sec. 2., we present our general formulation and detailed discussion of form factors for evaluating the differential and total cross sections of the  $\Delta$  resonance production following [11] emphasizing the minimal input, which is necessary. The numerical results are presented in Sec. 3.. In Sec. 4., we compare our model with electroproduction data from JLAB and finally give our conclusions in Sec. 5..

## 2. Neutrino production of $\Delta$ resonance

The invariant matrix element for charged current  $\Delta$  resonance production is written as

$$\mathcal{M} = \frac{G_F \cos \theta_c}{\sqrt{2}} j_\alpha \langle \Delta^{++} | V^\alpha - A^\alpha | p \rangle , \quad (1)$$

where  $V$  and  $A$  denote the hadronic weak vector and axial vector currents, respectively,  $\theta_c$  is the Cabibbo angle and  $G_F$  the Fermi constant. The matrix element of the leptonic weak current,  $j_\alpha$ , is

$$j^\alpha = \bar{u}_\mu \gamma^\alpha (1 - \gamma_5) u_\nu . \quad (2)$$

Following the notation of [5] we can express the matrix element as

$$\begin{aligned} \mathcal{M} = & \frac{G}{\sqrt{2}} \bar{\psi}_\alpha \left\{ \left[ \frac{C_3^V}{M_N} \gamma_\lambda + \frac{C_4^V}{M_N^2} (P_\Delta)_\lambda + \frac{C_5^V}{M_N^2} (P_p)_\lambda \right] \gamma_5 F^{\lambda\alpha} + C_6^V j^\alpha \gamma_5 \right. \\ & \left. + \left[ \frac{C_3^A}{M_N} \gamma_\lambda + \frac{C_4^A}{M_N^2} (P_\Delta)_\lambda \right] \gamma_5 F^{\lambda\alpha} + C_5^A j^\alpha + \frac{C_6^A}{M_N^2} q^\alpha q^\lambda j_\lambda \right\} u f(W) \end{aligned} \quad (3)$$

where  $F^{\lambda\alpha} \equiv q^\lambda j^\alpha - q^\alpha j^\lambda$ .  $\psi_\alpha$  is the Rarita-Schwinger spinor for the  $\Delta^{++}$  spin state,  $u$  is the Dirac spinor for the initial proton spin state,  $P_p$  is the four-momentum of the proton, and the S-wave Breit-Wigner factor  $f(W)$  can be written as follows

$$f(W) = \frac{\sqrt{\frac{\Gamma_\Delta(W)}{2\pi}}}{(M_\Delta - W) - \frac{1}{2}i\Gamma_\Delta(W)}, \quad \Gamma_\Delta(W) = \frac{\Gamma_\Delta^0 q_\pi(W)}{q_\pi(M_\Delta)} \quad (4)$$

with  $\Gamma(W) = \Gamma_0 q_\pi(W)/q_\pi(W_R)$  and  $\Gamma_0 = 120$  GeV. The  $C_j^V$  and  $C_j^A$  ( $j = 3, 4, 5, 6$ ) are the vector and axial vector form factors, respectively.

Due to the CVC the vector form factor  $C_6^V$  is zero and the other vector form factors can be determined from electroproduction experiments, where the magnetic form factor dominates. This leads to the following relations

$$C_4^V(Q^2) = -\frac{M}{W} C_3^V(Q^2) \quad \text{and} \quad C_5^V(Q^2) = 0. \quad (5)$$

This equation implies that electroproduction data depend only on the vector form factor  $C_3^V(Q^2)$ . Therefore, precise electroproduction data determine this form factor, which can be parameterized in various ways. Early theoretical work [13, 14] predicted the form factor to have a dipole form which was used to analyse neutrino scattering experiments [15, 16, 17]. However, subsequent electroproduction data [18, 19] showed that the magnetic  $N - \Delta$  transition form factor drops faster with increasing  $Q^2$  than the dipole form factor. Therefore, in our approach [11] we employ a modified dipole form for  $C_3^V$  giving an accurate representation:

$$C_3^V(Q^2) = \frac{C_3^V(0)}{\left[1 + \frac{Q^2}{M_V^2}\right]^2} \frac{1}{\left(1 + \frac{Q^2}{4M_V^2}\right)}. \quad (6)$$

Figure ?? shows data for the magnetic  $N - \Delta$  transition form factor  $G_M$ , divided by the dipole form factor  $G_D = 1/(1 + Q^2/M_V^2)^2$ , in dependence of  $Q^2$ . The solid curve, denoted 'PSY', shows our form factor in Eq. (6) and the dashed curve is the Sato-Lee form factor from Ref. [20]. One can see a clear deviation from the dipole form. Further details of the vector and axial vector contributions

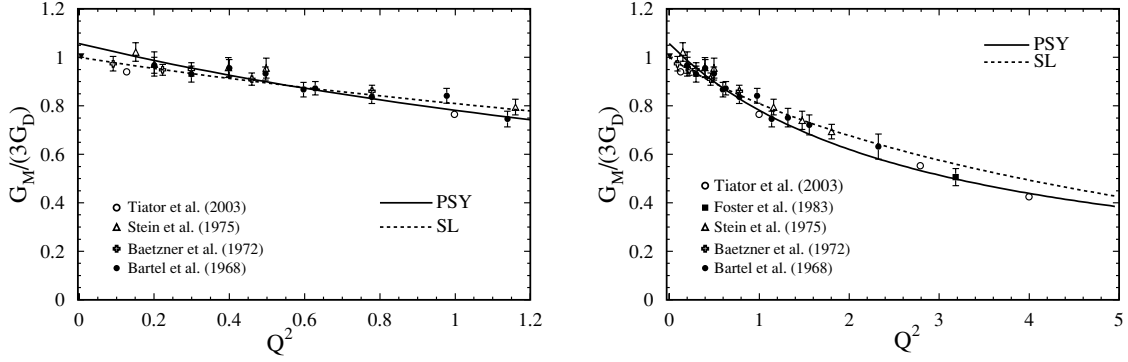


**Fig 1.** Magnetic  $N - \Delta$  transition form factor. The solid and dotted curves are the PSY FF [11] and the SL FF [20], respectively.

are discussed in section 3., where we will estimate the contribution of  $C_3^V$  from the electroproduction data.

We now turn to the axial vector form factors  $C_j^A$ , ( $j = 1, \dots, 6$ ). The PCAC condition gives the relation  $C_5^A(Q^2) = \frac{C_6^A}{M^2} Q^2$  which for small  $Q^2 = 0$  leads to the numerical value  $C_5^A(0) = 1.2$  [6]. The contribution of the form factor  $C_6^A$  to the cross section is proportional to the lepton mass and will be ignored. The  $Q^2$ -dependence of the form factors varies among the publications resulting in different cross sections and different  $Q^2$  distributions even when the same axial vector mass  $M_A$  is used. For this dependence we shall use again a modified dipole form

$$C_5^A(Q^2) = \frac{1.2}{\left[1 + \frac{Q^2}{M_A^2}\right]^2} \frac{1}{\left(1 + \frac{Q^2}{3M_A^2}\right)}. \quad (7)$$

For the other two form factors  $C_3^A(Q^2)$  and  $C_4^A(Q^2)$  we shall use  $C_3^A = 0$  and  $C_4^A(Q^2) = -\frac{1}{4}C_5^A$  [6]. It is evident that there is still some arbitrariness in the form factors with  $C_3^A$  and  $C_4^A$  being small.

The double differential cross section for  $\Delta$  resonance production is given by

$$\frac{d\sigma}{dQ^2 dW^2} = \frac{G_F^2}{16\pi M^2} \sum_{i=1}^3 [K_i W_i] \quad (8)$$

where  $G_F$  is the Fermi constant and  $M$  is the nucleon mass. The kinematic factors  $K_i(Q^2, E_\nu, W)$  and the structure functions  $W_i(Q^2, W)$  which are expressed in terms of helicity amplitudes are given in Ref. [6]. The helicity amplitudes depend on the Breit-Wigner factor in Eq. (4) and on the form factors  $C_j^V$ ,  $C_j^A$  which have been introduced already. In order to calculate the cross sections we need

the connection between the form factors  $C_j^V$ ,  $C_j^A$  and the helicity matrix elements ( $T$ 's and  $U$ 's). This relationship between them is discussed in Refs. [6, 11].

### 3. Results and discussions

The relative importance of the various form factors is shown in figure 2. One can see that  $C_3^V$  and  $C_5^A$  give the dominant contribution to the cross section. The cross section from the axial form factors has a peak at  $Q^2 = 0$ , while the cross section from  $C_3^V$  turns to zero. The zero from the vector form factor is understood, because in the configuration where the muon is parallel to the neutrino, the leptonic current is proportional to  $q_\mu$  and takes the divergence of the vector current, which vanishes by CVC. Since the contributions from  $C_4^V$  and  $C_4^A$  are very small the excitation of the  $\Delta$  resonance, to the accuracy of present experiments, is well described by two form factors  $C_3^V$  and  $C_5^A$ . Note that, since all form factors have been derived from photo- and electroproduction experiments in which a  $\Delta^+$  or a  $\Delta^0$  was produced, all the form factors need to be multiplied by  $\sqrt{3}$  in order to obtain the correct cross section for the  $\Delta^{++}$  production due to the fact that  $\langle \Delta^{++} | V_\alpha | p \rangle = \sqrt{3} \langle \Delta^+ | V_{em} | p \rangle$ .

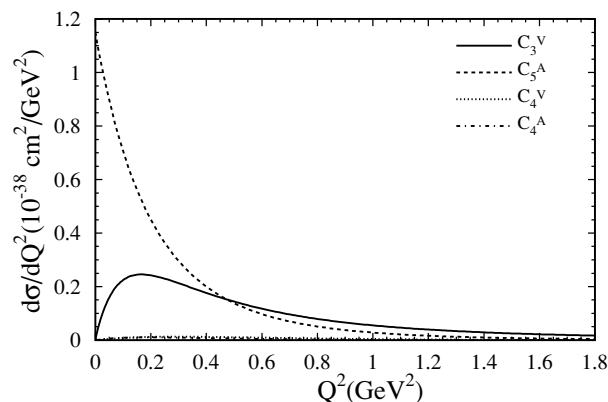


**Fig 2.** Partial cross sections proportional to the form factors in dependence of  $Q^2$ . The solid and dotted curves are the contributions proportional to the vector form factors  $C_3^V$  and  $C_4^V$ , respectively. The dashed and dot-dashed curves denote the parts proportional to the axial vector form factors  $C_5^A$  and  $C_4^A$ .

In addition, there are precise data for the electroproduction of the  $\Delta$  and other resonances [18], including their decays to various pion-nucleon modes, which allow to estimate the vector contribution. In the work of Galster et al. [18] cross sections for the channels  $(p + \pi^0)$  and  $(n + \pi^+)$  are tabulated from which we conclude that both  $I = 3/2$  and  $I = 1/2$  amplitudes are present. For instance, for  $W = 1.232$  GeV the  $I = 1/2$  background amounts about 10% of the cross section.

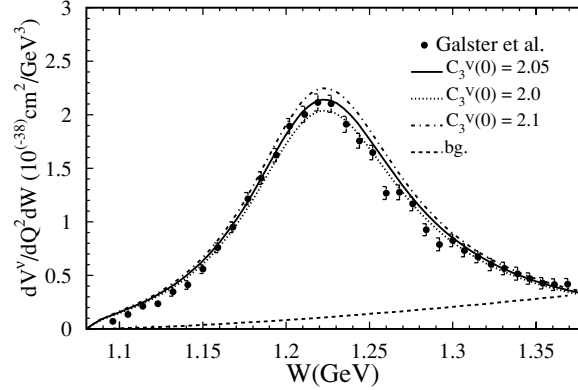


**Fig 3.** Cross section  $dV^\nu/dQ^2 dW$  for electroproduction in the  $\Delta$  resonance in comparison with Galster et al. data [18]. The solid, dotted and dot-dashed lines are obtained with  $C_3^V = 2.05$ ,  $C_3^V = 2.0$  and  $C_3^V = 2.1$ , respectively. The dashed line denotes the background contribution.

In Ref. [11], we performed a comparison with the electroproduction data after subtraction of the background, as shown in Fig. 3, and then used CVC to obtain the contribution of  $V_\mu^+$  to neutrino induced reactions using the formula

$$\frac{dV^\nu}{dQ^2 dW} = \frac{G^2}{\pi} \frac{3}{8} \frac{Q^4}{\pi\alpha^2} \frac{d\sigma^{\text{em}, I=1}}{dQ^2 dW} \quad (9)$$

to convert the observed [18] cross sections for the sum of the reactions  $e + p \rightarrow e + \begin{cases} p \pi^0 \\ n \pi^+ \end{cases}$  to the vector contribution in the reaction  $\nu + p \rightarrow \mu^- + p + \pi^+$  denoted in Eq. (9) by  $V^\nu$ . We used the data of Galster et al. [18] at  $Q^2 = 0.35 \text{ GeV}^2$  and subtracted the background as suggested by them. Subsequently, we converted the data points to the vector contribution for the neutrino reaction according to Eq. (9). The solid, dotted, and dot-dashed curves correspond to neutrino cross sections using a vector form factor  $C_3^V(Q^2)$  with  $C_3^V(0) = 2.05, 2.0, 2.1$ , respectively. The dashed line shows the contribution from the background. It is noteworthy that the analysis of the electroproduction data [18] included a contribution from the  $D_{13}(1520)$  resonance which was found to be small.

Next, we consider the  $Q^2$  distribution [21] from the Brookhaven experiment [22, 23], where the data have been presented as a histogram averaged over the neutrino flux and with an unspecified normalization. For the relative normalization, we normalized the area under the theoretical curve for  $Q^2 \geq 0.2 \text{ GeV}^2$  to the corresponding area of the histogram. In addition to the form factors for the  $\Delta$  resonance as described above we included a Pauli suppression factor in a simple Fermi gas model with Fermi momentum  $p_F = 0.16 \text{ GeV}$  [11]. The result is shown

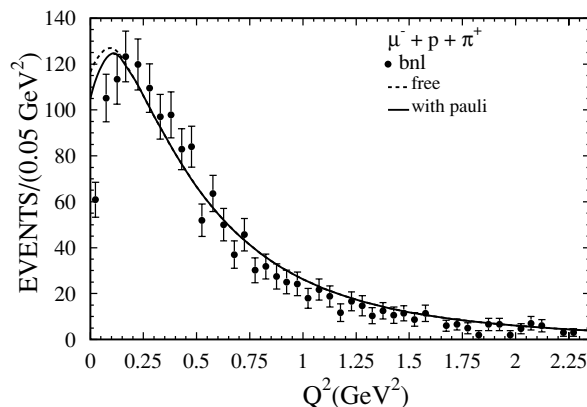


**Fig 4.**  $Q^2$ -spectrum of the process  $\nu p \rightarrow \mu^- p \pi^+$  in comparison with BNL data [22, 23]. The solid curve is with Pauli factor and dotted curve is free case.

as the solid curve in figure 4. The agreement is quite satisfactory. Performing a  $\chi^2$ -fit we obtained the following values for the free parameters

$$\begin{aligned} C_3^V(0) &= 1.95 & , & & C_5^A(0) &= 1.2 , \\ M_V &= 0.84 \text{ GeV} & , & & M_A &= 1.05 \text{ GeV} . \end{aligned} \quad (10)$$

For the entire  $Q^2$  region we found a  $\chi^2$  per degree of freedom of 1.76. Furthermore, in order to reduce nuclear effects we performed a fit to all data with  $Q^2 > 0.2 \text{ GeV}^2$  giving a  $\chi^2/d.o.f = 1.04$ . In the theoretical curves we averaged over the neutrino flux for the BNL experiment [24]. The dotted curve is the calculation without Pauli factor and the solid one with Pauli suppression factor included which has a small effect. It will be interesting to repeat this analysis as soon as new data become available. From Fig. 4 we can see that in the region of small  $Q^2$ , say  $Q^2 < 0.2 \text{ GeV}^2$ , the theoretical values are significantly above the experimental results which is not cured by a simple Pauli suppression factor.

To shed more light on this problem, it is reasonable to take the ratio of single pion production (RES) and quasi elastic scattering (QE) events,  $\frac{\sigma(\text{RES})}{\sigma(\text{QE})}$ . In Fig. 5 we show this ratio for total cross sections (left) and the  $Q^2$  distributions (right), respectively. The curves have been calculated with  $M_A = 1.05 \text{ GeV}$  and various values for  $C_5^A(0)$  and have been compared with BNL data [22]. Since the ratio reduces flux and experimental uncertainties it is an especially good test for a theoretical model. As can be seen from these figures we find very good agreement between our theoretical curves and the data, particularly also at low  $Q^2$ , say  $Q^2 < 0.2 \text{ GeV}^2$ , because uncertainties in the low  $Q^2$  region which are common to both, resonance and quasi-elastic scattering, drop out in the ratios. Comparisons

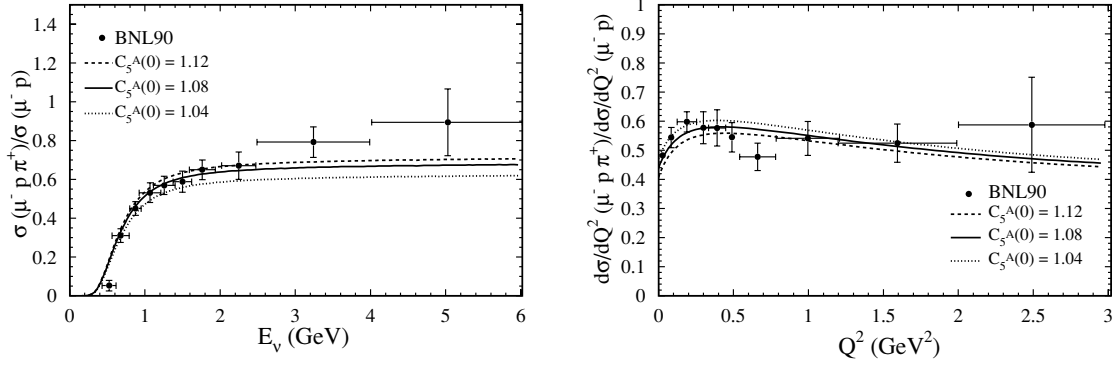


**Fig 5.** Ratio of the total cross section (left) and the  $Q^2$  distribution (right) for RES and QE in comparison with BNL data [22]. The solid, dotted, and dashed lines have been obtained with  $C_5^A = 1.08$ ,  $C_5^A = 1.04$ , and  $C_5^A = 1.12$ , respectively.

with other experimental data from BNL, FNAL, and CERN [22, 23, 25, 26] can be found in Ref. [11] where we compare these data with our form factors and older form factors given in [6].

#### 4. Pion electroproduction

To investigate pion electroproduction we first consider the fully differential cross section for neutrino reactions [6] given by

$$\begin{aligned} \frac{d^4\sigma}{dQ^2 dW^2 d\Omega_\pi^*} &= \frac{1}{\sqrt{4\pi}} \frac{d^2\sigma}{dQ^2 dW^2} \left( Y_0^0 - \frac{2}{\sqrt{5}} (\tilde{\rho}_{(33)} - \frac{1}{2}) Y_2^0 \right. \\ &\quad \left. + \frac{4}{\sqrt{10}} \tilde{\rho}_{(31)} \text{Re} Y_2^1 - \frac{4}{\sqrt{10}} \tilde{\rho}_{(3-1)} \text{Re} Y_2^2 \right) \end{aligned} \quad (11)$$

where the double differential cross section  $\frac{d^2\sigma}{dQ^2 dW^2} = N \sum_{i=1}^3 K_i \widetilde{W}_i$  can be found in Eq. (8). Furthermore,  $\tilde{\rho}_{(33)}$ ,  $\tilde{\rho}_{(31)}$ ,  $\tilde{\rho}_{(3-1)}$  are spin density matrix elements and  $Y_l^m(\theta_\pi, \phi_\pi)$  are spherical harmonic functions. This cross section can be easily converted to the electroproduction case by dropping axial vector parts and an appropriate change of the normalization factor:

$$\begin{aligned} \frac{d^4\sigma}{dQ^2 dW^2 d\Omega_\pi^*} &= \frac{N}{\sqrt{4\pi}} \left( \sum_{i=1}^3 K_i (\widetilde{W}_i - D_i \frac{(3 \cos^2 \theta_\pi^* - 1)}{2}) \right. \\ &\quad - 2\sqrt{3} \sin \theta_\pi^* \cos \theta_\pi^* \cos \phi_\pi^* (K_4 D_4 + K_5 D_5) \\ &\quad \left. - \sqrt{3} \sin^2 \theta_\pi^* \cos 2\phi_\pi^* (K_6 D_6) \right) \end{aligned} \quad (12)$$



with the normalization factor  $N = \frac{\pi\alpha^2}{2M^2Q^2}$ . Note that this cross section has contributions proportional to  $\cos 2\phi_\pi^*$ ,  $\cos \phi_\pi^*$  and a part independent of  $\phi_\pi^*$ , where  $\phi_\pi^*$  is the pion azimuthal angle. Further,  $\theta_\pi^*$  denotes the pion polar angle. The kinematic factors  $K_i$ ,  $i = 1, \dots, 6$  and the structure functions  $\widetilde{W}_i, D_i$  can be found in [6] and depend on the vector form factors introduced in Sec. 2.

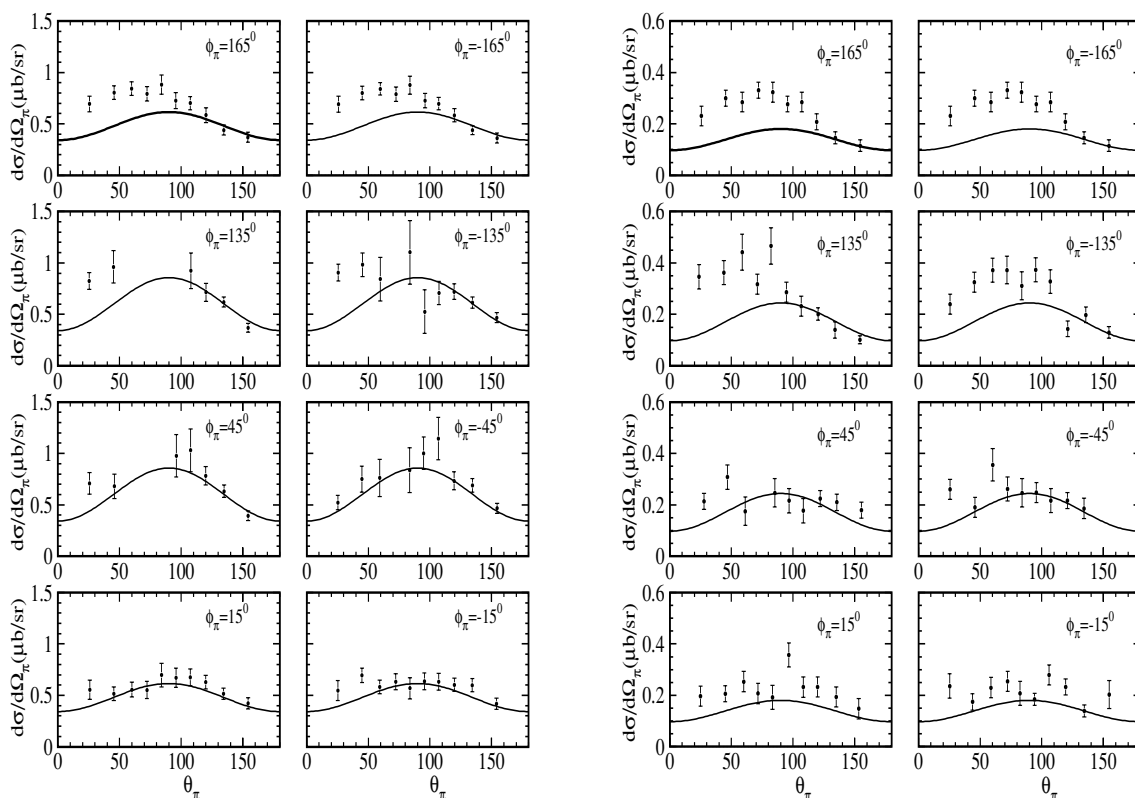


**Fig 6.** Electroproduction data [27] for  $Q^2 = 2.8 \text{ GeV}^2$  (left) and  $Q^2 = 4 \text{ GeV}^2$  (right), respectively, the reaction  $e + p \rightarrow e + p + \pi^0$ .

For our numerical comparison with electroproduction data we have calculated the fully differential cross section in Eq. (12) using the vector form factors given in Eqs. (5,6). In Fig. 6 we compare our results with JLab data for the reaction  $e + p \rightarrow e + p + \pi^0$  [27]. Shown is the dependence on the pion polar angle  $\theta_\pi$  for several azimuthal angles  $\phi_\pi$ , fixed  $W = 1.235 \text{ GeV}$ ,  $E_e = 3.2 \text{ GeV}$  and  $Q^2 = 2.8 \text{ GeV}^2$  (left) respectively  $Q^2 = 4 \text{ GeV}^2$  (right). With exception of the data points at  $|\phi_\pi| \geq 135^\circ$ , the description of the data by our simple model is quite satisfactory.

On the left side of Fig. 7, we show the  $\theta_\pi$  dependence for different values of

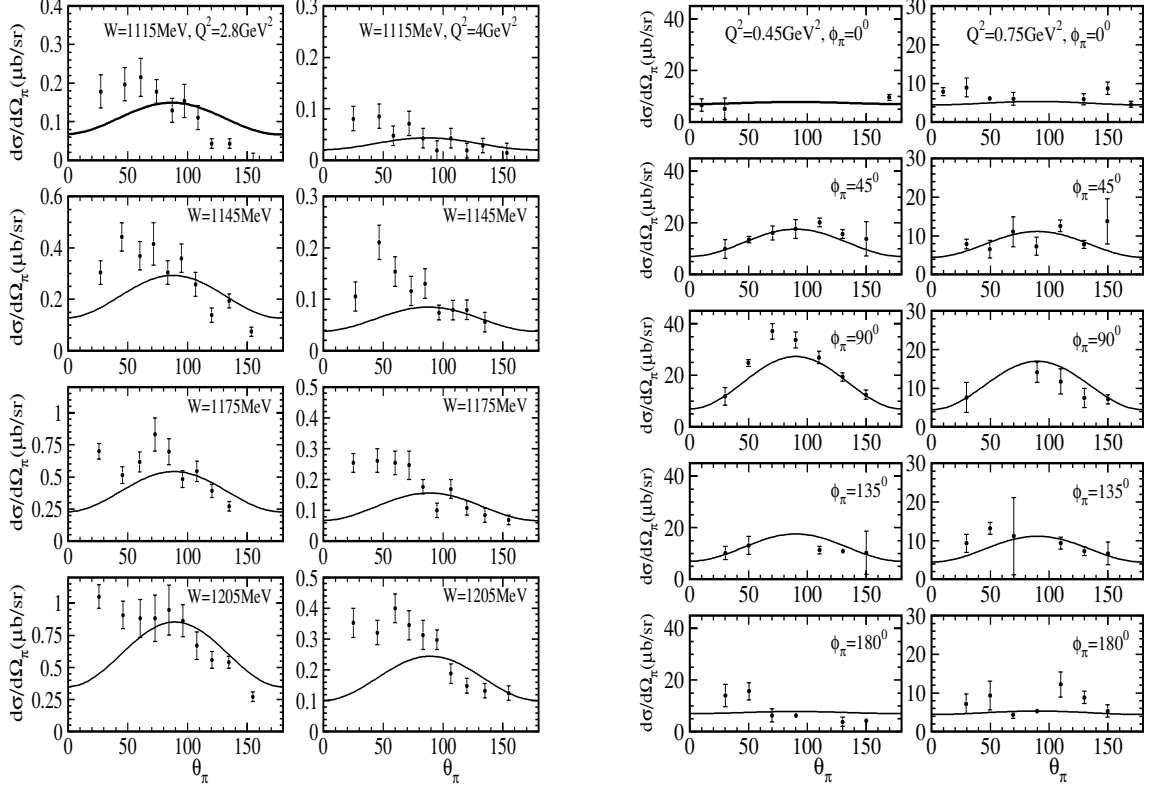


**Fig 7.** (Left) Dependence on  $\theta_\pi$  for different values of the  $\pi N$  invariant mass  $W$  for  $Q^2 = 2.8 \text{ GeV}^2$  and  $Q^2 = 4 \text{ GeV}^2$ . The data are from [27]. (Right) The same as in Fig. 6 for small momentum transfers  $Q^2 = 0.45 \text{ GeV}^2$  and  $Q^2 = 0.75 \text{ GeV}^2$ . The data points are from Ref. [28].

the  $\pi N$ -invariant mass  $W$  for  $Q^2 = 2.8 \text{ GeV}^2$  and  $Q^2 = 4 \text{ GeV}^2$ . The experimental results at different invariant mass  $W$  have been taken from [27]. Here, our results tend to undershoot the data in the region of small  $\theta_\pi$ . The right side of Fig. 7 shows the  $\theta_\pi$  dependence for different azimuthal angles  $\phi_\pi$ , for the region of small momentum transfers  $Q^2 = 0.45 \text{ GeV}^2$  and  $Q^2 = 0.75 \text{ GeV}^2$ . The data points are from Ref. [28]. One can see that at small momentum transfers the data are reasonably described even in the region of large azimuthal angles.

Before we leave this section it should be noted that the theoretical curves have been obtained without fine tuning of the parameter  $C_3^V(0)$ , for which we took the value  $C_3^V(0) = 2.0$ , and without including the background from the  $I = 1/2$  channel and a non-resonant background which is expected to be of the order of 10% at the resonance region.

## 5. Conclusions

We have shown that, at current experimental accuracy, the excitation of the  $\Delta$  resonance is well described by two form factors,  $C_3^V$  and  $C_5^A$ .  $C_3^V$  is consistent with electroproduction data and  $C_5^A$  can be determined only from neutrino data. Furthermore, relying on the connection of the weak vector current with the electromagnetic current due to the CVC condition we have compared the vector part of our formalism with electroproduction data.

In the future it will be interesting to include higher resonances and a non-resonant background and to perform a more detailed comparison with electroproduction data in order to study further the connection between neutrino- and electroproduction.

## Acknowledgments

I wish to thank the organizers of RCCN04 in Kashiwa/Japan for the kind invitation and financial support. I would like to thank E. A. Paschos, M. Sakuda, and I. Schienbein for their collaboration on the results presented here.

## References

- [1] M. Lindner, hep-ph/0503101.
- [2] C.H. Albright and L.S. Liu, *Phys. Rev.* **140** (1965) 748.
- [3] S.L. Adler, *Ann. of Physics* **50** (1968) 189.
- [4] P. Zucker, *Phys. Rev.* **D4** (1971) 3350.
- [5] C.H. Llewellyn Smith, *Phys. Rept.* **3** (1972) 261.
- [6] P.A. Schreiner and F. von Hippel, *Nucl. Phys.* **B58** (1973) 333.
- [7] G. L. Fogli and G. Nardulli, *Nucl. Phys.* **B160** (1979) 116.
- [8] G. L. Fogli and G. Nardulli, *Nucl. Phys.* **B165** (1980) 162.
- [9] D. Rein and L. Sehgal, *Ann. Phys.* **133** (1981) 79.
- [10] S. K. Singh, M. T. Vicente Vacas and E. Oset, *Phys. Lett.* **B416** (1998) 23.
- [11] E.A. Paschos, M. Sakuda and J.Y. Yu *Phys. Rev.* **D69** (2004) 014013; E.A. Paschos, M. Sakuda, I. Schienbein and J.Y. Yu, Proceedings of the 4nd International Workshop on Neutrino-Nucleon Interactions (NUINT04), published in *Nucl. Phys. Proc. Suppl.* **139** (2005) 125, hep-ph/0408185.
- [12] E.A. Paschos, L. Pasquali and J.Y. Yu, *Nucl. Phys.* **B588** (2000) 263; E.A. Paschos and J.Y. Yu, *Phys. Rev.* **D65** (2002) 033002; I. Schienbein and J.Y. Yu, Proceedings of the 2nd International Workshop on Neutrino-Nucleon Interactions (NUINT02), hep-ph/0308010; E.A. Paschos,

- D.P. Roy, I. Schienbein and J.Y. Yu, *Phys. Lett.* **B574** (2003) 232; Proceedings of the 2nd International Conference on Flavor Physics 2003 (ICFP2003), Korea, Seoul, October 2003, hep-ph/0312123; E.A. Paschos, I. Schienbein and J.Y. Yu, Proceedings of the 4th International Workshop on Neutrino-Nucleon Interactions (NUINT04), published in *Nucl. Phys. Proc. Suppl.* **139** (2005) 119, hep-ph/0408148.
- [13] S. Fubini, Y. Nambu and V. Wataghin, *Phys. Rev.* **111** (1958) 329.
- [14] R. H. Dalitz and D. G. Sutherland *Phys. Rev.* **146** (1966) 1180.
- [15] S.J. Barish et al., *Phys. Rev.* **D19** (1979) 2521.
- [16] G.M. Radecky et al., *Phys. Rev.* **D25** (1982) 1161.
- [17] T. Kitagaki et al., *Phys. Rev.* **D42** (1990) 1331.
- [18] W. Bartel et al. *Phys. Lett.* **B28** (1968) 148;  
S. Galster et al., *Phys. Rev.* **D5** (1972) 519;  
W. Bartel et al., *Phys. Lett.* **B35** (1971) 181.
- [19] L. Tiator et al. *Eur. Phys. J.* **A17** (2003) 357; S. Kamalow et al. *Phys. Rev.* **C64** (2001) 03221 and therein references.
- [20] T. Sato et al. *Phys. Rev.* **C67** (2003) 065201.
- [21] M. Sakuda in: NUINT 01 Conference, *Proc. Suppl. Nucl. Phys.* **112** (2002) 109, and E.A. Paschos, *ibid.* page 89.
- [22] T. Kitagaki et al., *Phys. Rev.* **D34** (1986) 2554.
- [23] K. Furuno, Talk at the 2nd Int. Conf. NUINT 02, Irvine, CA (Dec. 2002).
- [24] N.J. Baker, et al., *Phys. Rev.* **D23** (1981) 2499.
- [25] J. Bell, et al., *Phys. Rev. Lett.* **41** (1978) 1008.
- [26] G.T. Jones, *Z. Phys.* **C43** (1989) 527;  
D. Allasia et al., *Nucl. Phys.* **B343** (1990) 285.
- [27] V.V. Frolov et al, *Phys. Rev. Lett.* **82** (1995) 45.
- [28] R. Siddle et al., *Nucl. Phys.* **B35** (1971) 93;  
J. C. Adler et al., *Nucl. Phys.* **B46** (1972) 573.